The Journal of Chemical Physics

Covalent bonding in heavy metal oxides

Cite as: J. Chem. Phys. **146**, 134706 (2017); https://doi.org/10.1063/1.4979018
Submitted: 25 January 2017 . Accepted: 09 March 2017 . Published Online: 04 April 2017

Paul S. Bagus, Connie J. Nelin, Dave A. Hrovat, and Eugene S. Ilton

Covalent bonding in heavy metal oxides

Paul S. Bagus,[1] Connie J. Nelin,[2] Dave A. Hrovat,[1] and Eugene S. Ilton[3]
[1]*Department of Chemistry and the Center for Advanced Scientific Computing and Modeling, University of North Texas, Denton, Texas 76203-5017, USA*
[2]*Consultant, Austin, Texas 78730, USA*
[3]*Pacific Northwest National Laboratory, Richland, Washington 99352, USA*

(Received 25 January 2017; accepted 9 March 2017; published online 4 April 2017)

Novel theoretical methods were used to quantify the magnitude and the energetic contributions of 4f/5f-O2p and 5d/6d-O2p interactions to covalent bonding in lanthanide and actinide oxides. Although many analyses have neglected the involvement of the frontier d orbitals, the present study shows that f and d covalencies are of comparable importance. Two trends are identified. As is expected, the covalent mixing is larger when the nominal oxidation state is higher. More subtly, the importance of the nf covalent mixing decreases sharply relative to (n + 1)d as the nf occupation increases. Atomic properties of the metal cations that drive these trends are identified. *Published by AIP Publishing.* [http://dx.doi.org/10.1063/1.4979018]

I. INTRODUCTION

Covalent bonding in ionic crystals can be an important part of the interaction between the metal cations and the ligands; see, for example, Refs. 1–3. However, it is difficult to quantify the extent of covalency from experiment alone and theoretical calculations of the electronic structure are necessary. In particular, Mulliken population analyses[4–7] are commonly used to estimate covalent mixing in ionic materials from both band structure and molecular orbital, MO, calculations. For example, Mulliken population analysis, in conjunction with electronic structure calculations and ligand edge X-Ray Adsorption Spectroscopy, XAS, has been used to estimate the covalent character of heavy metal halides.[3,8] However, large uncertainties in the quantitative assignments of charges can occur,[9,10] especially when orbitals of different atoms participating in bonds strongly overlap. An alternative approach, Bader populations,[11] divides space into regions associated with each atom; however, this neglects the fact that regions of space are shared by nearby atoms. Another method, proposed by Weinhold and collaborators,[12,13] involves determining populations of special sets of orbitals called "natural orbitals." It is argued that the populations of these orbitals are less sensitive to the choice of basis sets than the conventional Mulliken analysis but uncertainties may still persist.[12]

Still another approach, introduced by Davidson,[14] is based on the projection of atomic orbitals onto the MOs of interest. We have used an extension of the "projection method" to analyze the covalent character of metal oxides and to estimate the uncertainties of the assigned charges.[15] The projection method also provides detailed information about the covalent contribution to the screening of core-level holes created during X-ray photoemission spectroscopy, XPS; see Refs. 15 and 16 and references therein.

With the projection method, it is possible to distinguish the covalent contributions of nf from (n + 1)d metal orbitals. In this regard, particularly in semi-empirical theoretical approaches, it is often assumed that the nf orbitals mix with the ligand orbitals for lanthanide and actinide oxides, whereas the (n + 1)d orbitals are neglected.[17,18] In contrast, the projection method has shown that the metal 5d and 6d orbitals for lanthanide and actinide oxides, respectively, also play major roles in covalent mixing.[15,16,19,20] Nonetheless, the magnitude of 5d/6d covalency is uncertain because the diffuse nd orbitals strongly overlap the ligand orbitals. Other recent work[3] also concluded that 6d covalent mixing is important for a wide variety of actinide complexes. Although a detailed analysis of symmetry concerning 5f and 6d covalency was provided, only a limited attempt was made to quantify the relative importance of 5f and 6d contributions to the overall covalent interaction. Thus, one of the major objectives of the present work is to establish the relative importance of the nf and (n + 1)d contributions.

In fact, none of the approaches mentioned above can determine the energetic importance of covalent interactions. There are, however, theoretical methods to decompose the properties of a system's wavefunction, WF, including the interaction energy, into contributions from different chemical and physical mechanisms;[21–25] For example, the constrained space orbital variation method, CSOV,[22,23] has been used to characterize bonding in Al_2O_3 and alkaline-earth oxides.[26] The CSOV method controls the variational space, for both occupied and unoccupied, or virtual, orbitals by freezing certain orbitals while allowing others to vary, thereby clearly distinguishing the chemical and physical effects that are included from those that are excluded. The constraints are equivalent to setting appropriate matrix elements of the effective Hamiltonian, or Fock operator, to zero. Moreover, it is possible with the CSOV method to explicitly select the terms to be included or excluded in a very general way. We stress that the CSOV method[22,23] and other methods to decompose the properties of WFs[24,25,27] are fully *ab initio* ways to separately determine the importance of different chemical and physical mechanism for these properties.

In previous work, the starting point for the constrained variations has been the superposition of the WFs for the fragments that are combined. In the present work, we have taken a different starting point to avoid the problem of working with an energetically unstable anion fragment. We begin with the best WFs where covalency has been explicitly excluded and then, progressively, turn on the covalency so that its energetic importance is explicitly addressed. We examine three U oxides with nominal oxidation states of U(VI), U(V), and U(IV) and two Ce oxides with nominal oxidation states of Ce(IV) and Ce(III). These choices allow us to examine how and why the nf shell occupation affects the energetics of the overall covalent interaction, as well as the relative importance of the nf and (n + 1)d contributions to covalency. The results are placed in the context of the competing atomic effects of nuclear attraction and Coulomb repulsion, which provides evidence for the general validity of our analysis.

In Sec. II, the theoretical methodology and the computational methods are briefly presented and reviewed. Section III is divided into several parts. First, we establish that the *ab initio* cluster model theory, which we use, provides an accurate description of the electronic structure of heavy metal oxides. Then, we use projection operators to estimate the extent of nf and (n + 1)d covalent character and address the uncertainties. We then quantify the energetic contributions of the covalent interaction using the CSOV energy decomposition method and demonstrate that the uncertainties are small in both the absolute sense and relative to the projection method. We conclude by summarizing the evidence that both nf and (n + 1)d covalent interactions are of comparable importance in heavy metal oxides and further that their relative and absolute importance is a strong function of the nf occupancy. In contrast to the Anderson model Hamiltonian approach[28–30] where the covalent character of the interaction, when it is considered, is accounted for in an indirect fashion,[19] this contribution treats the covalency directly. It also demonstrates that the MO theory provides a transparent way to understand covalent bonding in heavy metal oxides.

II. THEORETICAL METHODOLOGY AND COMPUTATIONAL DETAILS

Embedded UO_x and CeO_x cluster models were used to describe the oxides. Octahedral U(VI or V)O_6 clusters with O_h symmetry, see Fig. 1(a), were embedded in point charges that represent the extended environment of the crystal. The U(VI) cluster model geometry is based on the δ-UO_3 crystal and the U(V) cluster model geometry is taken as an average of more complex octahedral U(V) systems; the logic of these choices and the U-O distances, d(U-O), is described elsewhere.[16] Embedded U(IV)O_8 and Ce(IV or III)O_8 cluster models with the fluorite structure, see Fig. 1(b), were used, where d(cation-O) distances and the point charge placements were modeled after experimental structure determinations for UO_2 and CeO_2.[20,31] For Ce(III) an electron was added to the dominantly 4f shell, to represent a reduced impurity in CeO_2. Consequently, changes in covalent character are directly associated with the oxidation state and not convoluted with changes in the geometry. Furthermore, there is a strong evidence from a theoretical study of point defects in CeO_2[32] that the coordination of Ce(III) impurities is very similar to that of the Ce(IV).

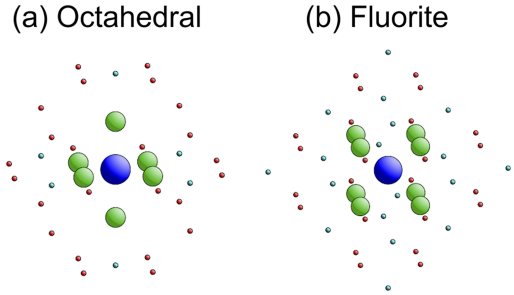

FIG. 1. The clusters used to model the (a) octahedral coordinated U(VI) and U(V), and (b) fluorite structure for CeO_2, and UO_2. The central cation and the nearest neighbor O anions are shown as large circles, and representative embedding point charges are shown as small circles.

The orbitals were variationally optimized as solutions of either 4-component Dirac Hartree-Fock,[33] DHF, or non-relativistic Hartree-Fock,[34] HF, equations. For the latter calculations, scalar relativistic effects were included through the use of effective core potentials,[35] ECP's, for the metal cations. Given open shell configurations, the orbitals were optimized for the average of configurations[33] where the electrons were distributed equally over all the open shell orbitals. However in order to study the properties of a WF for a multiplet with specific occupations of the open shell orbitals, WFs were constructed from configuration mixings over the determinants for all occupations of the individual open shell orbitals.[33] This is called a complete open shell configuration interaction, COSCI, which treats the angular momentum coupling and the covalent mixings induced by the ligand field on an equal footing.[19]

It will be useful for the later analysis of covalency to recall the general features of bonding and anti-bonding orbitals with schematic relations for these orbitals. The covalent mixing of the cation and ligand orbitals can be viewed as

$$\varphi_{\text{bond}} = [A\phi[O(2p)] + B\phi[X_\lambda]] \tag{1a}$$

and

$$\varphi_{\text{anti-bond}} = [-B\phi[O(2p)] + A\phi[X_\lambda]], \tag{1b}$$

where φ_{bond} denotes a fully occupied bonding orbital, $\varphi_{\text{anti-bond}}$ denotes an empty or partially occupied anti-bonding orbital,[19] $\phi[O(2p)]$ represents a suitable linear combination of O(2p) orbitals, and $\phi[X_\lambda]$ represents either a Ce 4f or 5d orbital, or a U 5f or 6d orbital. The simple relationships of Eq. (1) contain two important approximations. They assume that it is possible to rigorously define the $\phi[O(2p)]$ and $\phi[X_\lambda]$, which is only possible in a simple linear combination of atomic orbitals model, and they neglect the overlap of these orbitals, which is a major driving force for their covalent mixing. Neither of these approximations is used when the covalent mixing is rigorously determined through the solution of the HF and DHF variational equations. However, the schematic expressions of Eq. (1) do show the essential physics and chemistry of the bonding and anti-bonding orbitals. Thus, the choice of coefficients A and B, which neglects the overlap between $\phi[O(2p)]$ and $\phi[X_\lambda]$, demonstrates the orthogonality of the bonding and anti-bonding orbitals. For oxides, A > B so that the bonding orbitals are dominantly ligand and the anti-bonding orbitals

are dominantly metal cation. The bonding orbitals, φ_{bond}, are fully occupied while for closed shell Ce(IV) and U(VI) nominal oxidation states, the anti-bonding orbitals, $\varphi_{anti\text{-}bond}$, are empty. For the open shell nominal oxidation states of Ce and U, the $\varphi_{anti\text{-}bond}$ are partially occupied with 1 or 2 electrons. Since the cluster models are cubic, the cation nf and nd contributions to the cluster orbitals are separated by symmetry;[36] the nf orbitals belong to ungerade, u, representations and the nd orbitals belong to gerade, g, representations. It is clear from Eq. (1) that the actual charge on the cation, Q, will be less than the nominal oxidation state. The increase in the cation occupation from the term B for φ_{bond} is for a fully occupied orbital while the decrease in cation occupation from the term B for $\varphi_{anti\text{-}bond}$ is for an empty or partially occupied orbital. Indeed, one of our main objectives is to determine reliable estimates for the occupation of the cation frontier orbitals that arise from the covalent character of the cation-ligand interaction. However, while an occupation or a fragment orbital is a useful approximation, its value depends on the definition of occupation.[15] On the other hand, we will show that the energetic contributions of covalent mixings are much less uncertain as to their quantitative values.

Projection operators can be used to estimate the covalent character of an interaction.[15,37] For orbitals of suitable fragments, denoted φ^F, one defines projection operators, $\varphi^F\varphi^{F\dagger}$, and takes expectation values of the operator for the oxide cluster orbitals, denoted φ^C, to determine the fragment occupation of cluster orbital as $\langle\varphi^C|\varphi^F\varphi^{F\dagger}|\varphi^C\rangle$. The fragment orbitals of interest are the frontier d and f orbitals of the cation fragment and the orbitals with dominant 2p character for the O_6 and O_8 fragments. For the cation fragments, orbitals for the closed shell U^{+6} and Ce^{+4} ions define the projection operators. If we had used orbitals for different charge states of the cation fragments, we would have obtained slightly different projections. However, we have shown that the dependence of the projections on the choice of the ionicity used to determine the fragment orbitals is very weak; see also Ref. 38. By taking suitable sums over fragment orbitals and occupied cluster orbitals, one obtains an occupation of a group of fragment orbitals in the full set of occupied orbitals denoted as $N_P(F)$, where F denotes one of the fragments. The results are presented as departures from the nominal charges associated with the nominal oxidation state and are denoted $\Delta N_P(F)$. Of course, there is an uncertainty in these occupations because the pure fragment orbitals on the cation and anion overlap, and this leads to overestimates of the occupations, $N_P(F)$.[39] While corrections are possible,[14,39,40] they often just hide the extent of the uncertainty in the charge assignment. We prefer to estimate the uncertainty by comparing the projections of the cation orbitals and the O anion orbitals. Given conservation of electrons, the loss of charge from the anions should equal the gain in charge by the cations. In other words, for an ideal assignment,

$$\Delta N_P(X) = -\Delta N_P(O_n), \tag{2}$$

where X represents the cation frontier f or d orbital and O_n represents a suitable sum of g or u orbitals of the O fragment clusters. Departures from the equality of Eq. (2) indicate the uncertainty of the assignments of the projection charges.

Projection analysis does not provide information about the energetics of covalent mixing. In contrast, the CSOV method, which was originally formulated to characterize dative covalent bonding,[22,23] can be extended to specifically include or exclude covalent bonding between the ligand and the cation frontier f and d orbital, and thus determine their contributions to the interaction energy. The procedure is initially described for the closed shell U(VI) and Ce(IV) configurations. The first step of the CSOV process is to form a variational space which contains the occupied and virtual orbitals from HF calculations on the O_6 or O_8 and the Ce^{+4} or U^{+6} fragments, but where the frontier cations, Ce 4f and U 5f, and Ce 6d and U 6d, are explicitly excluded. If the full set of fragment occupied and virtual orbitals were retained, this would give results that are identical to the usual HF variational calculation in the space of the basis functions rather than that of the orbitals. However, since we exclude the Ce 4f and 5d or the U 5f and 6d orbitals from the variational space, this makes it impossible for them to participate in the cluster MOs; see Eq. (1). Hence, the HF orbitals in this reduced variational space are the best orbitals with the constraint that covalent mixing cannot occur. The determinantal WF formed with these orbitals is the step 0 WF. The second step, step 1a or V[nf + O2p], is to allow the frontier f orbital to mix with the closed shell occupied orbitals by using a reduced variational space that contains only the occupied optimized orbitals from step 0 and adding seven nf orbitals of the isolated cation to the variational space. Furthermore, only the occupied orbitals that have dominantly O(2p) character are allowed to vary; the other occupied orbitals are fixed as in the optimization at step 0. Thus, the only orbitals that can change at this step are those shown in Eq. (1a) where the cation orbitals, $\phi(X_\lambda)$, are restricted to be f orbitals. This variational constraint is equivalent to setting certain off-diagonal matrix elements of the Fock operator to 0. The energy lowering of the WF at this step is due entirely to the covalent mixing of O(2p) and the cation frontier f orbital. In the next partial step, denoted step 1b or V[nd + O(2p)], the only change is to add the five (n + 1)d orbitals to the variational space and to remove the seven nf orbitals such that only covalent bonding of O(2p) with the cation (n + 1)d orbitals is possible and bonding with nf is not allowed. Consequently, the energy lowering at this step is due entirely to covalent mixing between the O(2p) and the (n + 1)d orbitals. Next, the two previous steps are combined into a single step where both the five (n + 1)d orbitals and the seven nf orbitals are included in the variational space, denoted step 1(full) or V[nf&nd + O(2p)]. If the covalent mixing of the nf and the (n + 1)d were independent,[10] the energy lowering from CSOV step 0 to step 1(full) would be exactly equal to the sum of the energy lowerings from CSOV step 0 to step 1a and from step 0 to step 1b. In fact, as discussed later, there is some coupling between the cation nf and (n + 1)d covalent bonding with the O(2p). However, this coupling is weak, which permits separating the energetic importance of the covalent mixing of the O(2p) with the cation nf and (n + 1)d orbitals. There is also a coupling of the variation of the "spectator" orbitals with the variation of the orbitals involved in the covalent mixing of O(2p) and the frontier cation orbitals.[10] Determining the energetic importance of this coupling requires a second round of CSOV steps

0 and 1; however, the occupied orbitals at the starting point for the second pass are the orbitals determined for step 1(full) for the first pass. In this way, the spectator orbitals are readjusted to take into account the covalent bonding between the O(2p) and the cation nf and (n + 1)d. Repeating the series of CSOV steps 0 and 1 would yield the unconstrained variation results.[10] However, since the energy lowerings for the second pass are small compared to the first pass, further cycles are not necessary. This is another indication that the coupling of the different variations is weak. When we report the energy lowerings due to the covalent mixing of nf and (n + 1)d with O(2p), we sum the contributions over the energy increments for the two rounds of the steps 1.

The extension of the CSOV process for the open shell configurations is straightforward. At step 0, the closed shell orbitals are varied in the same occupied and virtual spaces as previously. However, one or two electrons are placed in the nf orbitals which were optimized for the isolated cation and then are frozen. This is done by setting the off-diagonal matrix elements of the Fock operator which connect the open shell nf orbital with other orbitals to zero. In the following CSOV steps, 1a, 1b, and 1(full), the only variational freedom is between the closed shell orbitals of dominantly O(2p) character with the open shell nf and (n+1)d orbitals taken from the WFs for the isolated cations. As before, the f and d covalencies are separated in steps 1a and 1b, respectively. For the (n + 1)d covalency only the bonding orbitals, represented in Eq. (1a), are occupied while for the nf covalency both the bonding, Eq. (1a), and the anti-bonding, Eq. (1b), orbitals are occupied. The orbitals are orthogonalized in the sequence (1) closed shell, (2) open shell orthogonalized to the closed shell, and (3) virtual, or unoccupied, orthogonalized to both the closed and open shell orbitals.

Calculations of the relativistic and non-relativistic WFs were performed with the DIRAC program system[41] and the CLIPS programs, respectively.[42] The relativistic WFs were all-electron calculations using large, uncontracted basis sets; see Refs. 16 and 19, and references therein. Relativistic calculations to obtain projections, for Ce(IV) and for U(IV) and U(VI), have been presented earlier.[15,19,20] However, in the present work, we use the same basis set parameters for the full set of oxidation states. Since these basis sets are somewhat different from those used in Ref. 15, there are minor differences in the numerical values presented here. For the non-relativistic WFs, the basis sets and (large core) ECPs for the metal cations were taken from the PNNL-EMSL tabulations.[43] For Ce and U the ECPs represented the 46 electron and the 78 electron cores, respectively, and the basis sets were not contracted. For O, an ECP was not used and the basis set had 9s and 5p elementary Gaussians contracted to 4s and 3p.[44] The CSOV calculations were performed with the non-relativistic CLIPS code and neglect the spin-orbit splitting, especially for the frontier f and d orbitals but take account of scalar relativistic effects through the use of pseudo-potentials.

III. RESULTS

A. Magnetic moment of UO_2

We show that the cluster model yields an accurate value for the magnetic moment of UO_2. The oxidation state of U in anti-ferromagnetic UO_2[45] is U(IV) with two electrons in the 5f open shell. For the isolated U^{4+} cation, the lowest level, or multiplet, is J = 4 which is 91% of the Russell-Saunders ^3H multiplet.[46] Taking account of the ligand field splitting in the O_h double group of UO_2, the J = 4 level is split and the lowest multiplet is a three-fold degenerate Γ_5 multiplet,[47] or a T_2 multiplet using Mulliken or Griffith notation.[48] The magnetic moment, μ, is given by

$$\mu = \langle L_Z \rangle + 2 \langle S_Z \rangle , \tag{3}$$

where the spin g-factor is taken as 2, L_z and S_z are the orbital and spin angular momenta in atomic units, and μ is in Bohr magnetons (μ_B).[49] The expectation values are taken for the direction z defined to give the maximum μ along z. The calculated values of the quantities in Eq. (3) for the lowest multiplets of U^{4+} and UO_2 are listed and compared to the experiment in Table I. For U^{4+}, the spin-orbit coupling to J = 4 is the principle reason that the angular momentum expectation values are reduced from the $\langle L_z \rangle = 5$ and $\langle S_z \rangle = 1$ found for the J = 6 coupling of the ^3H multiplet;[46] in particular, $\langle S_z \rangle < 0$ significantly reduces the value of μ. The value of μ is further reduced for UO_2, by about 40% leading to a value for μ quite close to experiment. The reduction of μ for UO_2 from the value for U^{4+} occurs largely because of the ligand field splitting of the 5f levels[50] but the covalent character of the open shells of UO_2 should also contribute. It is also possible with neutron scattering to determine the ratio of the orbital and spin contributions to the magnetic moment.[51] From Fig. 3 of Ref. 51, the ratio determined from the neutron experiments is estimated to be $\langle L_z \rangle/(2^*\langle S_z \rangle) = 3.15 \pm 0.15$. This is very close to the theoretical value of 3.08 for UO_2 from the data in Table I. The fact that the *ab initio* theoretical value of μ is only 10% larger than the experimental value and that the theoretical ratio of $\langle L_z \rangle/(2^*\langle S_z \rangle)$ is within experimental error indicates that our relatively simple UO_8 embedded cluster model for UO_2 and our Dirac-Fock CI WFs give an accurate description of the local electronic structure of UO_2. This includes the spin-orbit splittings, the intermediate coupling of spin and orbital angular momenta, and the covalent mixing of U 5f and O(2p). To place these results in context, a recent DFT + U band structure analysis of UO_2[52] yielded $\mu = 2.1\ \mu_B$ which is significantly further from experiment than the value of μ obtained with our cluster-based WF model. An earlier LDA + U calculation for UO_2[53] gave $\mu = 1.7\ \mu_B$ in excellent agreement with experiment but a ratio $\langle L_z \rangle/(2^*\langle S_z \rangle) = 1.9$, which is less than 2/3 of the experimental value.[51] Thus, it would appear that the cluster model and the *ab initio* WFs used in the present work are uniquely capable of describing both the total magnetic moment as well as the separate components

TABLE I. Magnetic moment, μ in μ_B, for U^{+4} and UO_2 compared to experiment. Values of the individual expectation values of orbital and spin angular momenta, $\langle L_z \rangle$ and $\langle S_z \rangle$, are also given.

	$\langle L_z \rangle$	$\langle S_z \rangle$	μ
U^{4+}	4.72	−0.72	3.28
UO_2	2.83	−0.46	1.92
Experiment[a]	...	...	1.74

[a]See Ref. 45.

from $\langle L_z \rangle$ and $\langle S_z \rangle$ with reasonable accuracy. Furthermore, our cluster model does not involve the need to make a choice of the parameter U.[52] Importantly, particularly in the context of this contribution, one can directly examine the covalent character of the localized orbitals using the cluster based WF model. Preliminary studies of PuO_2[54] indicate that *ab initio* cluster models and their WFs correctly describe yet another observable property of actinide compounds, namely, excitation energies. Such comparisons with experiment indicate that our approach should yield robust estimates for the extent and energetics of covalent mixing between cation and ligand frontier orbitals. While this covalent mixing is not directly accessible from experimental measurements, it is important to know the extent of this mixing in order to make reliable predictions of the properties of transition metal and actinide compounds.[8,55,56]

B. Projections of frontier orbitals for Ce and U oxides

Projections of the frontier f and d orbitals for the ground states of different oxidation states of Ce, Ce(III) and Ce(IV), and U, U(IV), U(V), and U(VI), are given in Table II. The projected occupations of the Ce 4f and 5d, the U 5f and 6d, and the O(2p) are presented as ΔN_P, the departure from the nominal occupations or oxidations. The O(2p) occupations are divided into $O(2p_g)$ where mixing with 5d (Ce) or 6d (U) is possible and $O(2p_u)$ where mixing with 4f (Ce) or 5f (U) is possible.

There is a modest f covalent mixing for closed shell Ce(IV), where the 0.3 electron 4f gain is similar to the increase in the 3d occupation for MnO over the occupation of five 3d electrons for the Mn(II) cation.[15] However, the loss of occupation of the $O(2p_u)$ due to covalent mixing with the Ce(4f), 0.1, is smaller than the gain in occupation of the Ce(4f) indicating that there is an uncertainty in the assignment of the Ce(4f) occupation. This is not surprising since the overlap of the Ce(4f) and O(2p) makes it difficult to distinguish whether charge belongs to Ce or O. The situation is rather different for Ce(III), see Table II, where the gain in occupation of Ce(4f), over the nominal value of 1, is much smaller than the gain for Ce(IV); furthermore, the loss of O(2p) occupation for Ce(III) is smaller than for Ce(IV). Consequently, the changes in Ce(4f) and O(2p) occupancies are consistent from Ce(IV) to Ce(III). This difference in the covalent character for the Ce(4f) of Ce(IV) and Ce(III) could, and indeed should, be related to the different catalytic activity of Ce(IV) and Ce(III).[57,58]

TABLE II. Projected departures, ΔN_P in electrons, from the nominal values given by the oxidation states for cation and anion occupations; see text for definitions of the various quantities.

	ΔN_P[Ce(4f)]	ΔN_P[O($2p_u$)]	ΔN_P[Ce(5d)]	ΔN_P[O($2p_g$)]
Ce(IV)	+0.31	−0.10	+2.51	−0.42
Ce(III)	+0.12	−0.06	+2.99	−0.38
	ΔN_P[U(5f)]	ΔN_P[O($2p_u$)]	ΔN_P[U(6d)]	ΔN_P[O($2p_g$)]
U(VI)	+1.40	−0.77	+2.99	−0.61
U(V)	+0.66	−0.37	+2.97	−0.61
U(IV)	+0.35	−0.09	+3.02	−1.16

Understanding the differences in the 4f covalency between Ce(IV) and Ce(III) in terms of a fundamental property of the Ce cations would help to establish general guidelines for the covalent behavior of other cations. Indeed, the following discussion demonstrates that atomic effects may be the dominant factor. There are two canceling atomic effects: (1) Coulomb repulsions within the compact Ce(4f) shell and (2) nuclear attraction which favors adding electrons to the Ce(4f) shell. The analysis uses a quantitative measure of the spatial extent of the cation and anion orbitals as given with $r(nl)_{Avg}$,

$$r(nl)_{Avg} = \left[\left\langle r(nl)^2 \right\rangle\right]^{1/2}, \tag{4}$$

where the expectation values are taken for isolated cation and anion orbitals averaged over the spin-orbit split components. The $r(nl)_{Avg}$ do not depend strongly on the charge state of the anion but they are taken for Ce^{4+} and O^{2-}. For Ce(4f), $r(4f)_{Avg}$ = 0.65 Å which is about 25% of the Ce-O distance in ceria. Since the 4f orbital is compact, there will be a large Coulomb repulsion between electrons within this shell. The magnitude of this Coulomb repulsion can be estimated from the F^0(4f,4f) Slater integral,[59] which, for the non-relativistic HF WF for Ce^{4+}, is F^0(4f,4f) = 23 eV. This rather large Coulomb repulsion within the 4f shell offsets the gain in energy from a larger nuclear attraction by being closer to the nucleus with a small r_{Avg}. The occupation of the 4f shell, given by N_P, can be taken as a rough guide to how large the Coulomb repulsion within the shell will be with the larger N_P having a larger Coulomb repulsion. Thus, there will be a much reduced 4f covalency for Ce(III) since here $N_P = 1 + \Delta N_P$. Indeed, it is easy to generalize this argument to the occupation of localized, contracted atomic shells in general as will be shown in the later discussion of covalency in U oxides.

The increase and decrease in occupancies for 5d and O(2p), respectively, for Ce(III) and Ce(IV), are much larger compared to their 4f-O2p counterparts (Table II), which suggests greater mixing compared to 4f. However, the magnitudes ΔN_P[Ce(5d)] and ΔN_P[O($2p_g$)] are far from equal. This reflects the large uncertainty arising from the strong overlap of the diffuse Ce(5d) with the $O(2p_g)$ orbitals, where $r(5d)_{Avg}$ = 1.4 Å plus $r[O(2p)]_{Avg}$ = 0.8 Å is almost equal to d(Ce–O) = 2.4 Å. Although the uncertainties could be reduced by making assignments of the "overlap" populations that force the equality of Eq. (2),[4–7,14,40] such assignments would be largely arbitrary. In contrast, we will show that the uncertainty concerning the importance of the covalency for the interaction can be resolved using the CSOV energy decomposition, as highlighted later.

Although the magnitudes of the projections for the covalent mixing for the different U oxidation states (Table II) do not satisfy the perfect equality of Eq. (2), ΔN_P[U(5f)] and ΔN_P[O($2p_u$)] change in a consistent manner as a function of U oxidation state, similar to ΔN_P[Ce(4f)] and ΔN_P[O($2p_u$)] for Ce. As expected, the more diffuse U(6d) orbitals, with r_{Avg}(6d) = 1.2 Å, show a much greater apparent covalent mixing as well as more uncertainty in occupancy assignments than for U(5f). Although there is appreciable covalent mixing of the metal frontier orbitals with O(2p), uncertainties in the projected occupancies, especially for (n + 1)d, preclude an accurate assignment of the extent of the covalent

mixing. Further, as noted earlier, the projections provide no information about the energetic contributions of these covalent mixings.

C. Energetic contributions of covalent mixing

The contributions to the interaction energy, that is the energy lowerings, obtained with the CSOV decomposition and its extensions, described in Sec. II, are given in Table III. The contributions, denoted ΔE[f + O(2p)] and ΔE[d + O(2p)], are the contributions at CSOV steps 1a and 1b where only mixing of the nf with $O(2p_u)$ or only mixing of nd with $O(2p_g)$ is allowed, respectively. The sums of these two energy lowerings are listed in Table III under the heading Sum(f + d). The total covalent contribution, denoted ΔE[f&d + O(2p)], is where the mixing of the nf and (n + 1)d is taken into account simultaneously in CSOV step 1(full). The difference between Sum (f + d), and ΔE[f&d + O(2p)] indicates the degree of coupling between the nf and (n + 1)d covalent mixings. If this difference is large, the division of the covalent energy lowerings into separate contributions from nf and (n + 1)d is uncertain. However, even in the most extreme case of U(VI), the difference between Sum(f + d) and ΔE[f&d + O(2p)] is only 15% (Table III). Thus, the separation into individual energy lowerings from nf and (n + 1)d covalency is valid.

The energy lowering, or energetic importance, due to the 4f covalency decreases substantially, by almost 66%, from Ce(IV) to Ce(III), while the energetic importance of the 5d covalency increases slightly by ∼15%. This is fully consistent with the projection results in Table II, but we are now able to quantify the energetic importance of the covalent mixing. For Ce(IV), the 4f and 5d covalencies are of comparable importance for the bonding, while for Ce(III), the covalent mixing of 4f with O(2p) is only about a third of that for the mixing of 5d with O(2p).

The energy contributions depend even more strongly on the different oxidation states for U. The 5f and 6d energy contributions both decrease markedly with decreasing nominal and effective oxidation states (Table III). This trend is due to the energetic cost of creating formally high cation oxidation states, which grows rapidly with increasing ionization.[60] Indeed, it is the covalent mixing that reduces the effective cation charge, thereby lowering the energetic cost of ionization. That the energy contribution of nf covalency decreases faster than for (n + 1)d as the nominal and effective nf occupations increase arises from the greater Coulomb repulsion between the compact nf electrons compared to that of the more diffuse nd electrons.

TABLE III. Energy contributions from covalent mixing of frontier cation orbitals with O(2p), ΔE in eV, for different oxidation states of Ce and U; see text for the definition of the ΔE.

	ΔE[f + O(2p)]	ΔE[d + O(2p)]	Sum(f + d)	ΔE[f&d + O(2p)]
Ce(IV)	0.94	0.96	1.90	1.89
Ce(III)	0.39	1.13	1.52	1.54
U(VI)	11.84	8.33	20.17	17.40
U(V)	4.30	4.28	8.58	7.68
U(IV)	1.23	2.15	3.39	3.27

An important result is that the CSOV determined energetic contribution of covalent mixing of cation (n + 1)d with ligand 2p orbitals cannot be neglected; it is comparable to the nf contribution. However, the projection method appears to indicate that the (n + 1)d contributions should be much larger than for nf (Table II). This discrepancy can be resolved by focusing on the uncertainties associated with each method. As discussed previously, the projection method yielded large uncertainties in the (n + 1)d occupancies (compare ΔN_P(cation) with the ΔN_P(anion) in Table II). This reflects the dangers of projections, in particular, and population analyses, in general, since they may have serious limitations and should be used with care, especially for making quantitative assignments; see also Refs. 9 and 10. In contrast, we place much greater faith in the CSOV decompositions which yielded clearer trends as a function of cation oxidation states, and lower uncertainties as demonstrated by the similar values for Sum(f + d) and ΔE[f&d + O2π] (Table III).

IV. CONCLUSIONS

The absolute and relative energetic importance of the covalent interactions involving 4f and 5d orbitals for lanthanides and 5f and 6d for actinides has been quantified using an extended CSOV decomposition method. Compelling evidence is presented that (n + 1)d covalent interactions are of comparable importance, sometimes even of greater importance, than for nf. In contrast, the projection method yields uncertain results, particularly for the (n + 1)d orbitals, because they strongly overlap the O2p orbitals.

The energetic contributions from covalent mixing increase as the nominal oxidation state of the cation becomes larger. This trend occurs because covalent mixing lowers the effective ionicity of the cation below that of its nominal oxidation state, thus reducing the energetic cost of ionizing the cation. The importance of this energetic cost is seen, for example, from the ionization potential of U^{+5} to U^{+6} which is over 60 eV.[60]

The importance of the nf covalency, as shown both by projection and by energy decomposition, decreases faster than for (n + 1)d as the occupation of the nf shell increases. This trend is due to the competition between the larger nuclear attraction of adding electrons to a compact orbital with a small $\langle r \rangle_{Avg}$ and the large Coulomb repulsion of electrons within this compact shell. This atomic effect is especially important for Ce and may be a factor determining the different catalytic activities of oxidized and reduced Ce.

ACKNOWLEDGMENTS

P.S.B. and E.S.I. acknowledge support from the U.S. Department of Energy, Office of Science, Office of Basic Energy Sciences, Chemical Sciences, Geosciences, and Biosciences (CSGB) Division through the Geosciences program at Pacific Northwest National Laboratory. We also acknowledge very helpful discussions with H.-J. Freund, especially for those relating to distinguishing oxidized and reduced Ce. Furthermore, we are grateful to G. H. Lander for providing helpful information about the magnetic moment of UO_2.

[1] P. A. Cox, *Transition Metal Oxides: An Introduction to Their Electronic Structure and Properties* (Clarendon Press, Oxford, 1992).
[2] J. S. Griffith, *The Theory of Transition-Metal Ions* (Cambridge Press, Cambridge, 1971).
[3] M. L. Neidig, D. L. Clark, and R. L. Martin, Coord. Chem. Rev. **257**, 394 (2013).
[4] R. S. Mulliken, J. Chem. Phys. **23**, 2338 (1955).
[5] R. S. Mulliken, J. Chem. Phys. **23**, 2343 (1955).
[6] R. S. Mulliken, J. Chem. Phys. **23**, 1833 (1955).
[7] R. S. Mulliken, J. Chem. Phys. **23**, 1841 (1955).
[8] S. G. Minasian *et al.*, J. Am. Chem. Soc. **134**, 5586 (2012).
[9] H. Chang *et al.*, Phys. Rev. B **49**, 15753 (1994).
[10] C. W. Bauschlicher, Jr. and P. S. Bagus, J. Chem. Phys. **81**, 5889 (1985).
[11] J. Hernandez-Trujillo and R. F. W. Bader, J. Phys. Chem. A **104**, 1779 (2000).
[12] A. E. Reed, R. B. Weinstock, and F. Weinhold, J. Chem. Phys. **83**, 735 (1985).
[13] A. E. Reed and F. Weinhold, J. Chem. Phys. **83**, 1736 (1985).
[14] E. R. Davidson, J. Chem. Phys. **46**, 3320 (1967).
[15] P. S. Bagus and C. J. Nelin, J. Electron Spectrosc. Relat. Phenom. **194**, 37 (2014).
[16] C. J. Nelin, P. S. Bagus, and E. S. Ilton, RSC Adv. **4**, 7148 (2014).
[17] A. Kotani, M. Okada, and T. Jo, Phys. Scr. **35**, 566 (1987).
[18] Y. Yamazaki and A. Kotani, J. Phys. Soc. Jpn. **60**, 49 (1991).
[19] P. S. Bagus, E. S. Ilton, and C. J. Nelin, Surf. Sci. Rep. **68**, 273 (2013).
[20] P. S. Bagus, C. J. Nelin, and E. S. Ilton, J. Chem. Phys. **139**, 244704 (2013).
[21] H. Umeyama and K. Morokuma, J. Am. Chem. Soc. **99**, 1316 (1977).
[22] P. S. Bagus, K. Hermann, and C. W. Bauschlicher, Jr., J. Chem. Phys. **80**, 4378 (1984).
[23] P. S. Bagus and F. Illas, J. Chem. Phys. **96**, 8962 (1992).
[24] P. R. Horn, Y. Mao, and M. Head-Gordon, J. Chem. Phys. **144**, 114107 (2016).
[25] P. R. Horn and M. Head-Gordon, J. Chem. Phys. **144**, 084118 (2016).
[26] G. Pacchioni *et al.*, Phys. Rev. B **48**, 11573 (1993).
[27] W. J. Stevens and W. H. Fink, Chem. Phys. Lett. **139**, 15 (1987).
[28] K. Okada, A. Kotani, and B. T. Thole, J. Electron Spectrosc. Relat. Phenom. **58**, 325 (1992).
[29] A. Kotani and T. Yamazaki, Prog. Theor. Phys. Suppl. **108**, 117 (1992).
[30] A. Kotani and H. Ogasawara, Phys. B **186-188**, 16 (1993).
[31] R. W. G. Wyckoff, *Crystal Structures* (Wiley, New York, 1963).
[32] A. M. Burow *et al.*, J. Chem. Phys. **130**, 174710 (2009).
[33] L. Visscher *et al.*, Comput. Phys. Commun. **81**, 120 (1994).
[34] C. C. J. Roothaan, Rev. Mod. Phys. **32**, 179 (1960).
[35] T. R. Cundari and W. J. Stevens, J. Chem. Phys. **98**, 5555 (1993).
[36] G. Burns, *Introduction to Group Theory with Applications* (Academic Press, New York, 1977).
[37] C. J. Nelin, P. S. Bagus, and M. R. Philpott, J. Chem. Phys. **87**, 2170 (1987).
[38] P. S. Bagus *et al.*, Phys. Rev. Lett. **58**, 559 (1987).
[39] P. S. Bagus and F. Illas, Phys. Rev. B **42**, 10852 (1990).
[40] J. Knut Faegri and T. Saue, J. Chem. Phys. **115**, 2456 (2001).
[41] DIRAC, "A relativistic *ab initio* electronic structure program," Release DIRAC08, written by L. Visscher, H. J. Aa. Jensen, and T. Saue, with new contributions from R. Bast, S. Dubillard, K. G. Dyall, U. Ekström, E. Eliav, T. Fleig, A. S. P. Gomes, T. U. Helgaker, J. Henriksson, M. Iliaš, Ch. R. Jacob, S. Knecht, P. Norman, J. Olsen, M. Pernpointner, K. Ruud, P. Sałek, and J. Sikkema, see the URL at http://dirac.chem.sdu.dk, 2008.
[42] CLIPS is a program system to compute *ab initio* SCF and correlated wavefunctions for polyatomic systems. It has been developed based on the publicly available programs in the ALCHEMY package from the IBM San Jose Research Laboratory by P. S. Bagus, B. Liu, A. D. McLean, and M. Yoshimine.
[43] The URL for the EMSL basis set data is http://bse.pnl.gov/bse/portal.
[44] P. S. Bagus, G. Pacchioni, and F. Parmigiani, Chem. Phys. Lett. **207**, 569 (1993).
[45] J. Faber and G. H. Lander, Phys. Rev. B **14**, 1151 (1976).
[46] P. S. Bagus *et al.*, Chem. Phys. Lett. **546**, 58 (2012).
[47] G. Amoretti *et al.*, Phys. Rev. B **40**, 1856 (1989).
[48] R. Boca, *A Handbook of Magnetochemical Formulae* (Elsevier, Amsterdam, 2012).
[49] N. W. Ashcroft and N. D. Mermin, *Solid State Physics* (Holt, Rinehart, and Winston, NY, 1976).
[50] H. U. Rahman and W. A. Runciman, J. Phys. Chem. Solids **27**, 1833 (1966).
[51] G. H. Lander, M. S. S. Brooks, and B. Johansson, Phys. Rev. B **43**, 13672 (1991).
[52] F. Zhou and V. Ozolins, Phys. Rev. B **83**, 085106 (2011).
[53] S. L. Dudarev *et al.*, Micron **31**, 363 (2000).
[54] P. S. Bagus and R. L. Martin, "Theoretical analysis of the electronic structure and magnetic properties of PuO_2" (to be published).
[55] F. A. Cotton and G. Wilkenson, *Advanced Inorganic Chemistry* (Wiley, New York, 1972).
[56] A. E. Clark *et al.*, J. Phys. Chem. A **109**, 5481 (2005).
[57] *Catalysis by Ceria and Related Materials*, edited by A. Trovarelli (Imperial College Press, London, UK, 2002).
[58] Y. Pan *et al.*, Phys. Rev. Lett. **111**, 206101 (2013).
[59] J. C. Slater, *Quantum Theory of Atomic Structure, Vols. I and II* (McGraw-Hill, New York, 1960).
[60] C. E. Moore, "Atomic energy levels," National Bureau of Standards No. 467 (U.S. GPO, Washington, DC, 1952), see also URL http://physics.nist.gov/cgi-bin/AtData/main_asd.